J. Fluid Mech. (1972), *vol.* 55, *part* 4, *pp.* 629–639
Printed in Great Britain

Water-drop response to sudden accelerations

By P. G. SIMPKINS
Bell Laboratories, Whippany, N.J.
AND E. L. BALES
Stevens Institute of Technology, Hoboken, N.J.

(Received 4 May 1972)

The deformation of initially spherical drops of radius r_0 subjected to an external flow of velocity u is experimentally examined for a large range of Weber and Bond numbers. Observations of the changes in the response are compared with recent analytical predictions. The data show that beyond a critical Weber number the response ceases to be vibratory and becomes monotonic with time. Subsequently, it is found that, although the response is unstable, the deformation imposed by the external aerodynamic pressure distribution remains the dominant factor. Measurements of the drag coefficient yield a mean value of $C_D = 2{\cdot}5$ over a large Reynolds-number range. The time at which Taylor instability occurs is shown to be inversely proportional to Bond number to the one-quarter power. There is little evidence of the instability occurring until a normalized time $t^* = (\epsilon^{\frac{1}{2}}\bar{t}u/r_0)$ is approximately unity; here ϵ is the gas/liquid density ratio (ρ/ρ') and $\bar{t}$ is the real time.

1. Introduction

When a drop with a surface tension σ is exposed to an external flow, a critical value of the Weber number $We = \rho u^2 r_0/\sigma$ is reached at which the drop ceases to vibrate and undertakes a monotonic deformation. This transition occurs when the applied aerodynamic pressure forces exceed the restoring forces due to surface tension. The original work on the vibratory response of drops is discussed in Lamb (1932), and numerous experiments have demonstrated that the fundamental frequency ω_0 agreed well with Rayleigh's (1879) result, $\omega_0 = (2\sigma/\pi^2\rho' r_0^3)^{\frac{1}{2}}$. Using a linearized model, Hinze (1948) demonstrated that when the distortion is of $O(2r_0)$ the breakup of a drop is dependent on We. Hinze's criterion for the critical distortion can, however, only be considered as an empiricism since it has little foundation in a linearized theory.

Harper, Grube & Chang (1972) have shed new light on the drop response phenomena in a unified theory based on modern perturbation methods. These authors have illustrated that the acceleration imparted to a drop will ultimately cause the windward surface of the drop to become susceptible to Taylor instability (see Taylor 1950). The transition between the simple distortion and the deformation accompanied by unstable surface waves which grow exponentially with time is characterized by the Bond number $Bo = \rho' g r_0^2/\sigma$, where g is the

acceleration. Bo is related to We by Newton's law in the form $Bo = \frac{3}{8}C_D\,We$, where C_D is the drag coefficient. The results from numerical experiments in Harper *et al.* (1972) show that the instability effects begin when $Bo \approx 11$. However, because the surface-wave growth rate is small, the deformation due to the non-uniform pressure distribution dominates the response even at $Bo \sim O(10^3)$. This regime, in which the deformation occurs in the presence of unstable, long-wavelength surface waves is defined as being quasi-stable, and the numerical results suggest that it persists up to $Bo \simeq O(10^5)$. Eventually, the drop response is acceleration dominated and the unstable Taylor waves pierce the drop before it has sufficient time to distort.

So many experimental studies of drop response have been reported for various liquids that we shall only cite representative results. Lane (1951) conducted the earliest comprehensive study and reported observations of drops of a bag-like appearance in steady wind-tunnel flows, and a viscous shearing effect in transient shock-tube flows. From these observations, Lane erroneously concluded that the bag-like response phenomenon only occurred in steady flows for $2{\cdot}1 < We < 4{\cdot}8$. Later, Hanson, Domich & Adams (1963) observed the bag-like response in a series of shock-tube experiments, and also noted that at slightly greater relative velocities the drop developed an umbrella-like appearance with a re-entrant stem. In these experiments the value of the critical Weber number varied from 3·6 to 7·1. Most other investigations, such as Engel's (1958), were done in the quasi-stable region where instability effects, if they did indeed occur, only became apparent towards the latter stages of the response. In such circumstances the drop profile becomes considerably obscured and only qualitative estimates could be made of when the fragmentation occurred. Reinecke & Waldman (1970), using flash X-ray techniques, have obtained data for Bond numbers greater than 10^4, and made estimates of the breakup time from microdensitometry traces of the X-ray plates. This is the only study in which quantitative information of the breakup time has been obtained, for large Bond numbers.

The present experiments were primarily intended to examine the dynamic response of drops for $Bo > 10^3$, although data will be given for lower Bond numbers. Particular attention has been given to establishing the value of the drag coefficient of the distorting drops, since this is inherent in determining the appropriate Bond number for the tests. It is important to note that the theory of Harper *et al.* (1972) is valid in regions where the initial surface displacement is small, so that the stability analysis can be linearized. In reality such situations only occur at very high Bond numbers, of $O(10^5)$, where the initial algebraic deformation is minimized, and the induced acceleration dominates the dynamic response of the drop. We shall see that at moderate values of Bo the response continues to be dominated by the algebraic response due to the non-uniform aerodynamic loading, even though the drop is unstable to windward surface disturbances.

2. Predictions of transient response

The classical solution for small amplitude vibrations (see Lamb 1932) predicts that the frequency is given by

$$\omega_{n-2} = \{(n-1)\,n(n+2)\,\sigma/4\pi^2\rho' r_0^3\}^{\frac{1}{2}}. \tag{1}$$

This equation reduces to the Rayleigh fundamental frequency when $n = 2$, and is equivalent to the result for $Re \to \infty$ derived by Hinze. The recent perturbation expansion (Harper *et al.* 1972) leads to the linearized result for the surface displacement of the drop:

$$\frac{r}{r_0} = \eta = 1 + \epsilon \sum_{n=0}^{\infty} \frac{n(2n+1)}{4\beta_n^2} C_n P_n(\mu)\,[\cos\beta_n t - 1] + O(\epsilon^2). \tag{2}$$

Here, the C_n are coefficients evaluated from the surface pressure distribution, and the $P_n(\mu)$ are zonal harmonics, where $\mu = \cos\theta$ and t the normalized time $(\bar{t}u/r_0)$. Equation (2) describes the vibration of a drop with a normalized frequency

$$\beta_n = \{(n-1)\,n(n+2)/We'\}^{\frac{1}{2}} \tag{3}$$

in terms of the small parameter ϵ and a modified Weber number

$$We' = \rho' u^2 r_0/\sigma \equiv (We/\epsilon).$$

The first two terms of the series are of no consequence since they represent a uniform compression and translation, respectively. For the special case when the free stream is a potential flow with zero circulation, the surface pressure distribution contains only the $P_2(\mu)$ mode and (2) reduces to

$$\eta = 1 + \tfrac{5}{16} C_2 \epsilon We' P_2(\mu)\{\cos(8/We')^{\frac{1}{2}}t - 1\}. \tag{4}$$

The results of a small-time co-ordinate expansion derived earlier by Harper, Grube & Simpkins (1970) are embedded in (4) and may be recovered by expanding for $We' \gg 1$. This yields

$$\eta = 1 - \tfrac{3}{4}\epsilon P_2(\mu) t^2 + O(1/We'), \tag{5}$$

a result also found by Burgers in an appendix to Engel's work.

From the above discussion we see that when the aerodynamic forces dominate the surface tension, i.e. $We' \gg 1$, a drop undertakes monotonic deformation with time. The interactions between the flow and the drop which occur near this so-called critical Weber number are nonlinear because the drop distortion is comparable to its initial radius. Ultimately it is in this region that the bag- and umbrella-type responses are observed. Recent experiments by Simpkins (1971) have indicated some limits of the different responses, typical photographs of which are shown in figure 1 (plate 1). An extension of the above analysis to account for nonlinear effects will be the subject of a further paper in which an estimate of the critical Weber number will be given.

All available experimental evidence indicates that the critical Weber number is less than the value at which the drop becomes unstable. In Harper *et al.* (1972) the lowest critical value of Bo is estimated to be about eleven, thus if $C_D = 1{\cdot}0$ the drop becomes unstable when $We > 30$. The principal features of the instability

analysis are similar to Taylor's (1950) original results on interfacial instability. The effect is purely inertial and occurs at the interface of a heavy fluid when it is accelerated by a lighter one pushing against it. Surface tension always plays a stabilizing role by damping any very small wavelength irregularities. For large Bond numbers the calculations of Harper *et al.* (1972) show the boundary between stable and unstable waves to occur at a wavenumber

$$n_c \propto Bo^{\frac{1}{2}} + O(1). \tag{6}$$

Below this cut-off wavenumber, all waves are unstable and exhibit an exponential growth rate proportional to $Bo^{\frac{1}{4}}$. Each wave grows at a different rate and a maximum occurs at the wavenumber

$$n_{\max} \propto (\tfrac{1}{3}Bo)^{\frac{1}{2}} + O(1). \tag{7}$$

Consequently, the time t_b required for break-up, due to unstable surface waves, is predicted by Harper *et al.* (1972) as

$$t_b = \bar{t}(g/r_0)^{\frac{1}{2}} \propto Bo^{-\frac{1}{4}}. \tag{8}$$

The magnitude of the proportionality constant is unspecified by the theory.

3. Experimental methods

A constant-area double-diaphragm shock tube 76 mm in diameter was used to drive shock waves at a freely falling stream of uniformly distributed water drops which issued from a hypodermic needle. The drop generator was a modified version of Dabora's (1967) design which had been made vacuum tight. A spring-loaded valve in the capilliary supply prevented damage due to the excess pressure behind the shock. This system produced drops ranging from 0·8 to 3 mm in diameter simply by changing the hypodermic needles.

The tests were carried out in air and argon atmospheres using helium and hydrogen driver gases, respectively. For high Bond numbers the driven tube was evacuated to between 25 and 3600 Torr after it had been flushed twice with dry test gas. The hydrogen–argon combination was used because it is the most efficient means of obtaining high-speed shocks. Thin-film heat gauges monitored the shock speeds, which were recorded with submicrosecond counters. The shock strengths were measured with piezo-electric transducers on a 150 MHz oscilloscope. At the highest shock speed, $M_s \doteq 9{\cdot}0$, approximately 500 μs of test time was available.

Optical records of the drop response were taken either as single- or multi-frame shadowgraph pictures. The single-frame data were acquired using Nikon 180 mm f2·8 lens with a 10 × 13 mm studio camera, giving an image magnification of 3 on the film. Illumination was produced by a 6·5 joule air spark flash tube of 0·5 μs duration. A signal from an upstream pressure transducer was supplied to a variable-time delay generator the output of which triggered the light source. Thus, photographs could be taken at various times after the incident shock wave had passed the drop.

Multiple-frame records of individual tests were taken with an image converter

camera at rates between 5×10^4 and 10^6 pictures/s. Ten pictures of the event were recorded, usually at 2×10^5 frames/s. The camera was equipped with a 152 mm lens and extension tubes producing magnifications of 3. The resolution is sufficient to enable the development of the drop response to be easily identified. For these tests a light source with 1 ms duration at constant intensity was used to illuminate the sequence of events.

4. Photographic observations

We have described how for a large range of Bond numbers the dynamic response of a drop may be described as quasi-stable. This phenomenon is illustrated by the motion pictures shown in figure 2 (plate 2), where a 1·2 mm drop at $Bo \approx 30$, conditions which exceed the critical values, shows no evidence of instability. Notice the very large distortion which occurs because of the nonlinear interaction with the free stream. Ultimately, liquid filaments are shed from the periphery of the distorted drop, which finally disintegrates.

The series of pictures shown in figure 3 (plate 3) at $Bo = 1{\cdot}37 \times 10^4$ exhibits a typical quasi-stable response; in figure 3(*c*) the distortion is accompanied by mass loss due to viscous shearing. Much later, in figure 3(*d*), we see that the drop has been displaced about five diameters and has been strongly affected by the flow field. Surface waves are now evident and an extensive region of mist scatters the incident light.

As the Bond number is increased further the instability occurs earlier. Two sets of pictures from the image converter camera, at identical flow conditions, are shown in figure 4 (plate 4). The onset of instability can be identified at about 25 μs. The front-lighted pictures, figure 4(*b*), show surface detail not evident in the shadowgraph records. In these pictures the field of view is limited to some 7×7 mm, consequently the complete response cannot be observed after about 25 μs. Still pictures in this Bond number regime have been taken, and do not exhibit any unexpected peculiarities. The drop shatters shortly after the instability occurs, the results appearing to be similar to those shown in figure 3(*d*) but occurring substantially earlier.

5. Drag coefficient measurements

The determination of drag coefficients for distorting drops presents difficulties which do not occur in free-flight drag measurements for rigid bodies. Provided that the drop profile is distinguishable, the centre-of-mass displacement rate can be observed and a drag coefficient determined. Gunn & Kinzer (1949) have shown that for vibrating drops or ones with small distortion the drag coefficients are similar to the rigid-sphere data at the corresponding Reynolds number. When the induced acceleration of the drop is large, however, the distortion is accompanied by surface stripping which obscures the leeward profile. The effect of the viscous shearing is twofold: (i) the drop mass is no longer conserved and (ii) the centre of mass cannot be located. To overcome these difficulties the drag coefficient is derived from measurements of the stagnation-point displacement

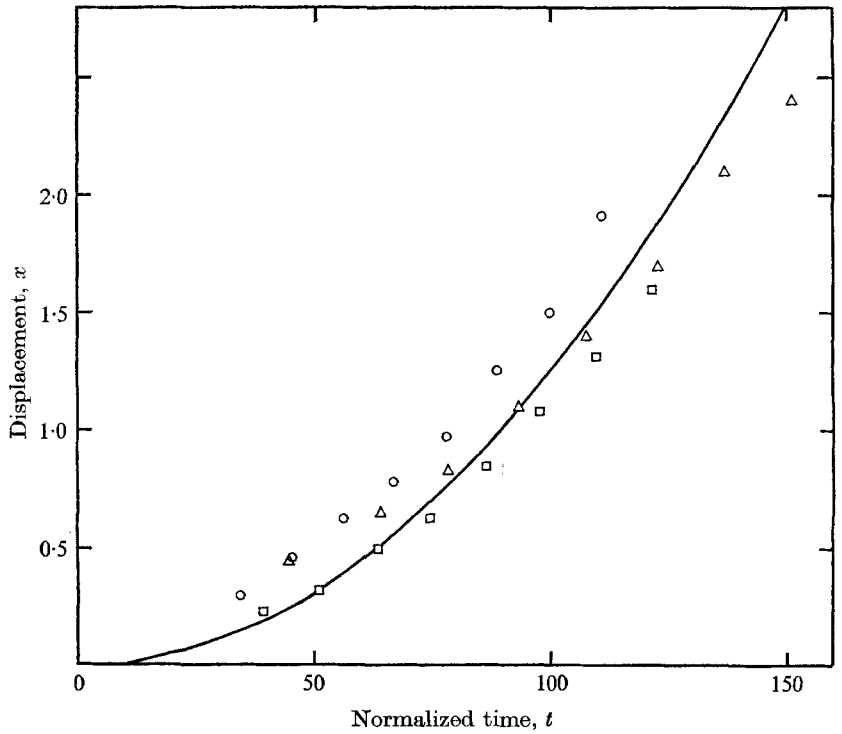

FIGURE 5. Drop displacement in air at $Bo \simeq 7{\cdot}6 \times 10^4$. $M_s = 6{\cdot}0$, $\epsilon = 0{\cdot}25 \times 10^{-3}$. △, $Re_d = 0{\cdot}81 \times 10^4$; □, $Re_d = 1{\cdot}06 \times 10^4$; ○, $Re_d = 1{\cdot}08 \times 10^4$; —, $x = 1{\cdot}25 \times 10^{-4} t^2$, $C_D = 2{\cdot}70$.

rate. Such estimates imply that the drag is larger than in reality since the effects of mass loss and distortion are explicitly neglected. Under these conditions the distorting drops exhibit a constant acceleration up to fragmentation. Under such an assumption, Newton's law yields the induced displacement in normalized co-ordinates as

$$x = \tfrac{1}{2}\epsilon g^{(1)} t^2,$$

where the acceleration is related to the drag coefficient by $g^{(1)} = \frac{3}{8}C_D$. Figure 5 shows displacement data measured from different tests; the solid line represents a mean parabola from which the drag coefficient is deduced. The resolution of the image converter data enabled measurements to be made to within 25 μm. The results from more than sixty data shots were condensed onto curves similar to those in figure 5 to obtain the drag data discussed below.

Most of the available drag coefficient data from the literature on deforming drops have been collated and are presented in figure 6. The shock-tube experiments show that the drag coefficient is substantially greater than the compressible-flow rigid-sphere value of $C_D = 1{\cdot}0$. For free-stream Mach numbers between one and four, the limited information on supersonic flow over rigid disks suggests that this is not unreasonable. Howarth (1953) indicates that drag coefficients vary between 1·8 and 2·8 for disks in compressible flows, a result substantially in agreement with the data in figure 6.

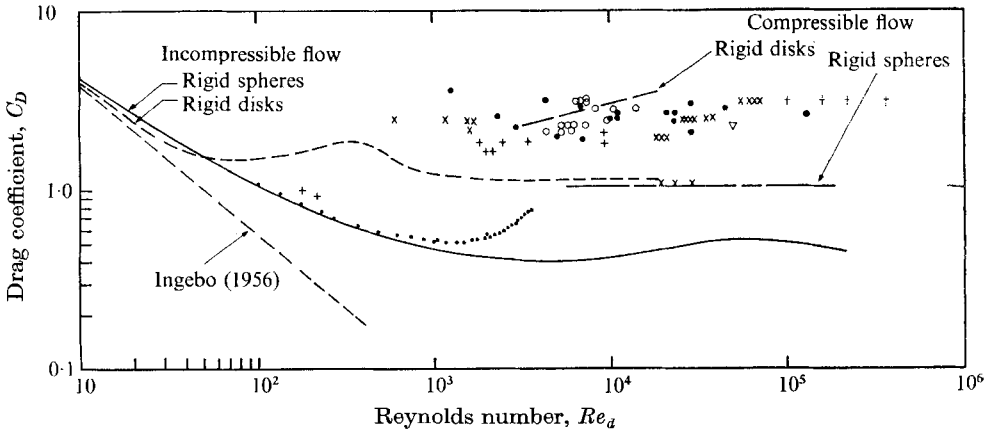

FIGURE 6. Drag coefficient of distorting water drops. Present results: ○, air; ×, argon. +, Rabin *et al.* (1960); ●, Jaarsma & Derksen (1967); †, Ranger & Nicholls (1969); ▽, Reinecke & Waldman (1970); •, Gunn & Kinzer (1949).

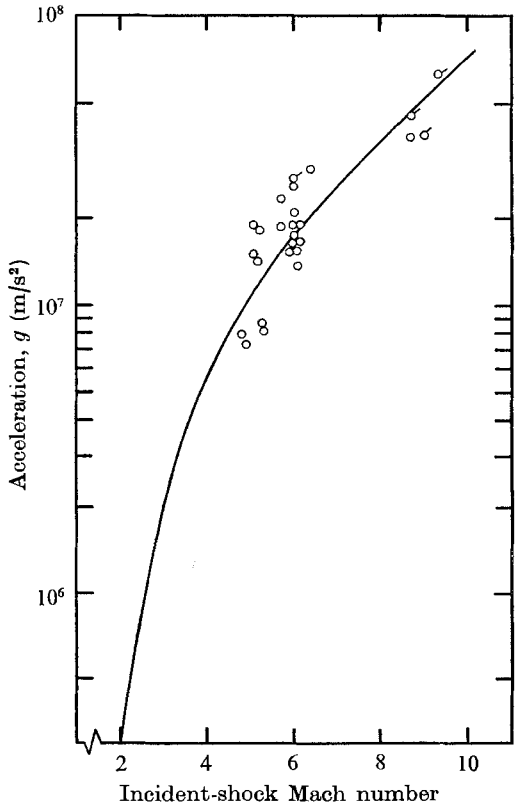

FIGURE 7. Shock-induced acceleration of 1 mm drops. —, $g = 0{\cdot}8\epsilon u^2/r_0$. Repeated data points are flagged. Results normalized to an initial pressure $p_1 = 1$ atmosphere.

In a note stimulated by Lane's work, Taylor (1949) estimated that the acceleration imparted to a lenticular drop could be expressed as

$$g = 3\varepsilon u^2/D, \quad \text{where} \quad D \simeq 3{\cdot}76 r_0.$$

This expression has been used to calculate the acceleration of a 1 mm drop when it is subjected to a shock wave in air at atmospheric conditions (NTP). The results are shown in figure 7 compared with the experimental observations which have been normalized to NTP conditions. Notice the extremely large values typical of the accelerations imposed on the drops in these circumstances and which are the driving mechanism for the interfacial instability. For example, at a shock Mach number of five, the acceleration $g \sim O(10^7\,\mathrm{m/s^2})$. The agreement between Taylor's prediction and the experimental results is surprisingly good, bearing in mind the simplifications made by Taylor to deduce the result.

6. Instability effects

More than fifty image converter records have been examined for evidence of instability effects, defined by an appearance and subsequent growth of surface waves on the windward side of the drops. Such information is inherently qualitative, but the uncertainty is usually bounded to within 5 μs, i.e. one frame on the camera record. The results are given in figure 8 as a function of Bond number. The normalized time t has been scaled by $\epsilon^{\frac{1}{2}}$ to eliminate changes in the initial shock-tube condition. These variations are inherent in the magnitude of the error bars, which correspond to 5 μs. Because the unstable modes are amplified selectively, deviations from an initially spherical drop result in the appearance of surface waves at some time different from that for the ideal case.

The data show that when $Bo < 5 \times 10^4$ there is very little evidence of instability effects for $t^* < 1{\cdot}0$. This result supports the conclusion (Harper *et al.* 1972) that the appearance of instability occurs when $t \sim O(\epsilon^{-\frac{1}{2}})$. The general trend of data is proportional to $Bo^{-\frac{1}{4}}$, and a least-square fit given by

$$t_0^* = 22 Bo^{-\frac{1}{4}}$$

is a reasonable representation of the onset criteria. As we have seen above, once the effects of instability manifest themselves the growth rate of the surface waves is exponential and subsequently, therefore, fragmentation occurs extremely rapidly.

Three data points given by Reinecke & Waldman (1970) for the breakup time, determined by X-ray absorption measurements, are shown in figure 8. The X-ray data, which do not contain uncertainty estimates, are in good agreement with the present measurements. The constant of proportionality in the expression for the breakup is about twice as large as the value estimated for the onset of the instability.

All the calculations involving the surface tension have used properties appropriate to normal temperature and pressure. In the experiments the ambient conditions are not atmospheric and the suitable physical conditions for the surface are unknown; however they will differ appreciably since the temperature

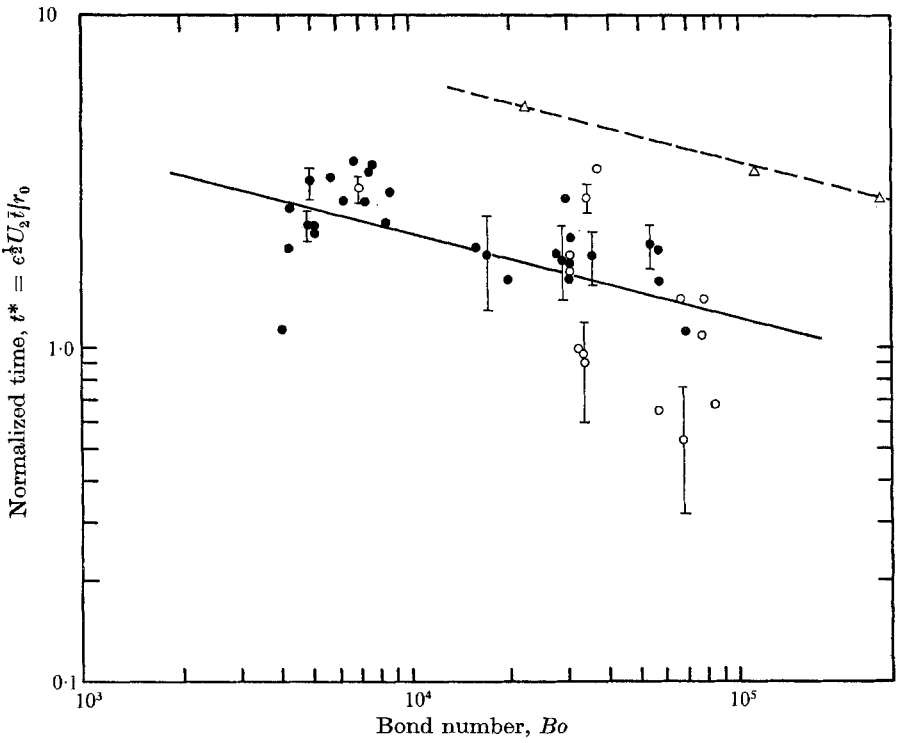

FIGURE 8. Onset of unstable surface waves. —, $t^* = 22\ Bo^{-\frac{1}{4}}$; – – –, estimated breakup time, $t^* = 65\ Bo^{-\frac{1}{4}}$. Experimental results: ●, argon, present results; ○, air, present results; △, Reinecke & Waldman (1970).

and pressure are both altered substantially. For the pressure levels of interest, compressibility effects are small, but the variations in surface tension due to temperature changes may be large. Moreover, the surface tension is affected even though the bulk of the liquid preserves its original temperature and only the surface layer is heated. Such behaviour can be expected to occur in the experimental environment because the thermal inertia of the drop keeps it cooler than the shock-heated gas. By solving the heat-conduction equation one can show that the temperature of the drop will not alter significantly during the test time. However, since the forced convective heating to a rigid body in such circumstances is important, it is not unreasonable to expect the surface temperature of the drop to increase. Then, if $\sigma_\tau = \sigma_0(1-\gamma\theta)$, where θ is the temperature, Partington (1962) suggests that the coefficient $\gamma \simeq 2{\cdot}33\alpha$, where $\alpha = 1{\cdot}95 \times 10^{-4}\ (°C)^{-1}$ is the coefficient of thermal expansion at 20 °C. From this result we anticipate that for moderate shock speeds, i.e. $M_s < 2$, the surface tension would change by less than 10 %. The change in the Bond number due to a modification of this size would therefore not alter the experimental results significantly.

When the shocks are stronger, say $M_s = 6$, a large temperature difference occurs which will alter the surface tension. The magnitude of this change must remain open to question at present since the rate of heat transfer to the liquid is unknown. The effect will be to increase the value of Bo above the results quoted

here. Consequently, the observations of instability occurring at Bond numbers greater than 5×10^3 supports the contention in Harper *et al.* (1972) that unstable surface waves dominate the response when $Bo \sim O(10^5)$.

7. Conclusions

In summary the principal results are as follows.

(i) The drop response is algebraic when $7 < We < 50$. In this region the non-linear coupling between the deforming drop and the external flow results in a phenomenon which is characterized by either a bag- or umbrella-like response.

(ii) The drag coefficient for distorting drops is similar to the rigid-sphere value for $Re_d < 10^3$. When compressibility effects become significant a mean value of $C_D = 2{\cdot}5$ is observed for $10^3 < Re_d < 10^5$. The latter result is comparable to measurements taken from rigid disks in similar flow conditions.

(iii) Measurements of the drop acceleration compare very well with Taylor's prediction for a lenticular drop.

(iv) Although the drop is unstable beyond $Bo \simeq 11$ there is no evidence of instability effects until Bo is much greater, say 10^4. This observation supports the conclusion drawn from numerical experiments that a large quasi-stable region where the deformation rate dominates the interfacial instability exists.

(v) For values of $Bo < 4 \times 10^5$ there is no evidence of instability effects when $t^* < 1{\cdot}0$.

(vi) The onset of Taylor instability is found to be approximated by the relationship $t^* = 22Bo^{-\frac{1}{4}}$. This result represents the lower bound for estimates of the breakup time and is consistent with the observations of Reinecke & Waldman.

We wish to thank Dr E. Y. Harper for numerous helpful discussions and Dr O. G. McKee for his enthusiastic support. Mr R. C. McCrea assisted with the experiments. The work was performed while one of us (E. L. B.) was a summer consultant at Bell Laboratories.

REFERENCES

Dabora, E. 1967 *Rev. Sci. Instrum.* **28**, 502.

Engel, O. 1958 *J. Res. N.B.S.* **60**, 245.

Gunn, R. & Kinzer, G. D. 1949 *J. Meteor.* **6**, 243.

Hanson, A. R., Domich, E. G. & Adams, H. S. 1963 *Phys. Fluids*, **6**, 1970.

Harper, E. Y., Grube, G. W. & Chang, I. D. 1972 *J. Fluid Mech.* **52**, 565.

Harper, E. Y., Grube, G. W. & Simpkins, P. G. 1970 *Proc. 3rd Int. Conf. Rain Erosion and Ass. Phenomena.* (Ed. A. A. Fyall & R. B. King), p. 405.

Hinze, J. O. 1948 *Appl. Sci. Res.* A **1**, 263, 273.

Howarth, L. 1953 *Modern Developments in Fluid Dynamics, High Speed Flow*, vol. 2, p. 722. Oxford University Press.

Ingebo, R. D. 1956 *N.A.C.A. Tech. Note*, no. 3762.

Jaarsma, F. & Derksen, W. 1967 *N.R.L. Rep.* no. 251 (unpublished).

Lamb, H. 1932 *Hydrodynamics*, 6th edn., p. 475. Cambridge University Press.

LANE, W. R. 1951 *Ind. Eng. Chem.* **43**, 1312. (See also *Surveys in Mechanics* (ed. G. K. Batchelor). Cambridge University Press.)

PARTINGTON, J. R. 1962 *Advanced Treatise on Physical Chemistry*, vol. 2, p. 150 *et seq.* Longmans.

RABIN, E., SCHALLENMULLER, A. & LAWHEAD, R. B. 1960 *A.F.S.O.R. Tech. Rep.* 60–75 (unpublished).

RANGER, A. A. & NICHOLLS, J. A. 1969 *A.I.A.A. J.* **7**, 285.

RAYLEIGH, LORD 1879 *Proc. Roy. Soc.* A **29**, 71.

REINECKE, W. R. & WALDMAN, G. 1970 *Proc. 3rd Int. Conf. Rain Erosion & Ass. Phenomena*, (ed. A. A. Fyall & R. B. King), p. 629.

SIMPKINS, P. G. 1971 *Nature*, **233**, 37.

TAYLOR, G. I. 1949 *Scientific Papers*, vol. 3, p. 457, Cambridge University Press.

TAYLOR, G. I. 1950 *Proc. Roy. Soc.* A **201**, 192.

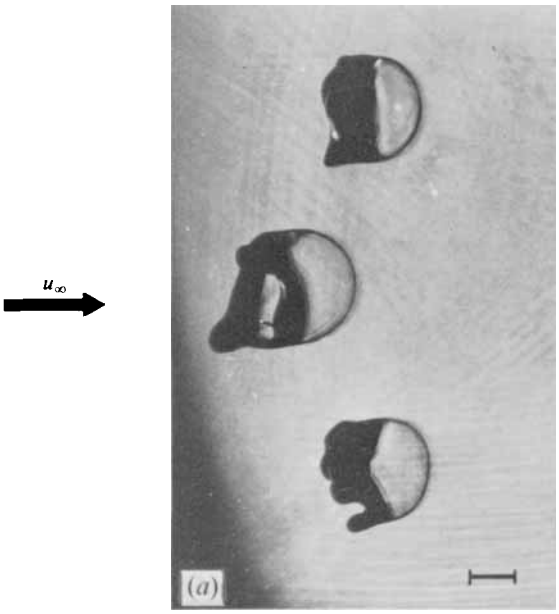

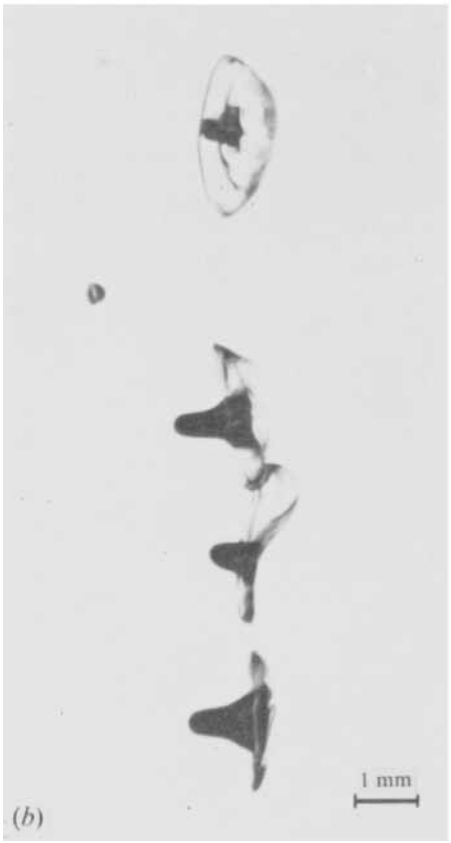

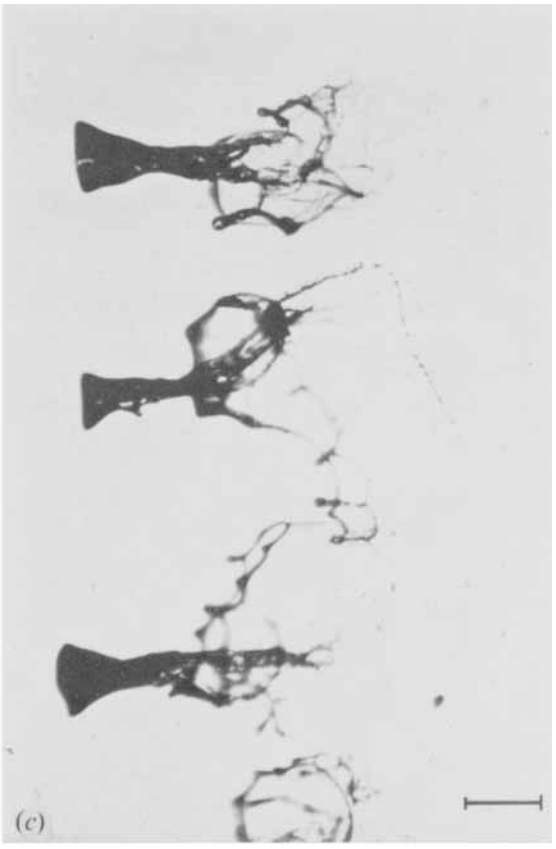

FIGURE 1. Nonlinear response phenomena. (*a*) The bag at $We = 10$, $\bar{t} = 1280\ \mu$s. (*b*) The umbrella at $We = 45$, $\bar{t} = 1385\ \mu$s. (*c*) The umbrella at $We = 45$, $\bar{t} = 1570\ \mu$s.

SIMPKINS AND BALES (*Facing p.* 640)

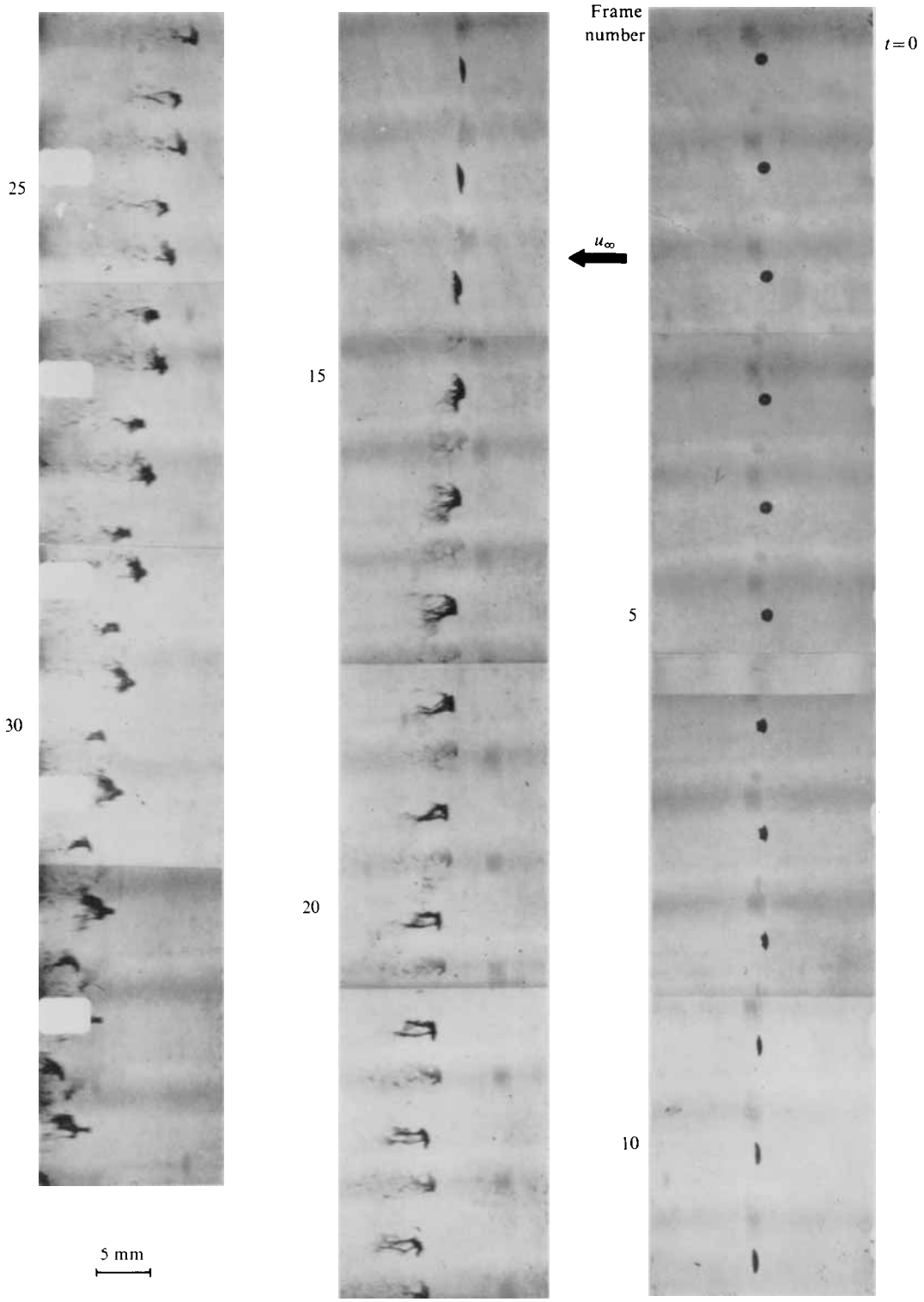

FIGURE 2. Dynamic response of a 1·2 mm drop near to the critical Bond number. $Bo \simeq 30$, $Re_d = 4560$, framing rate = 12 000/s.

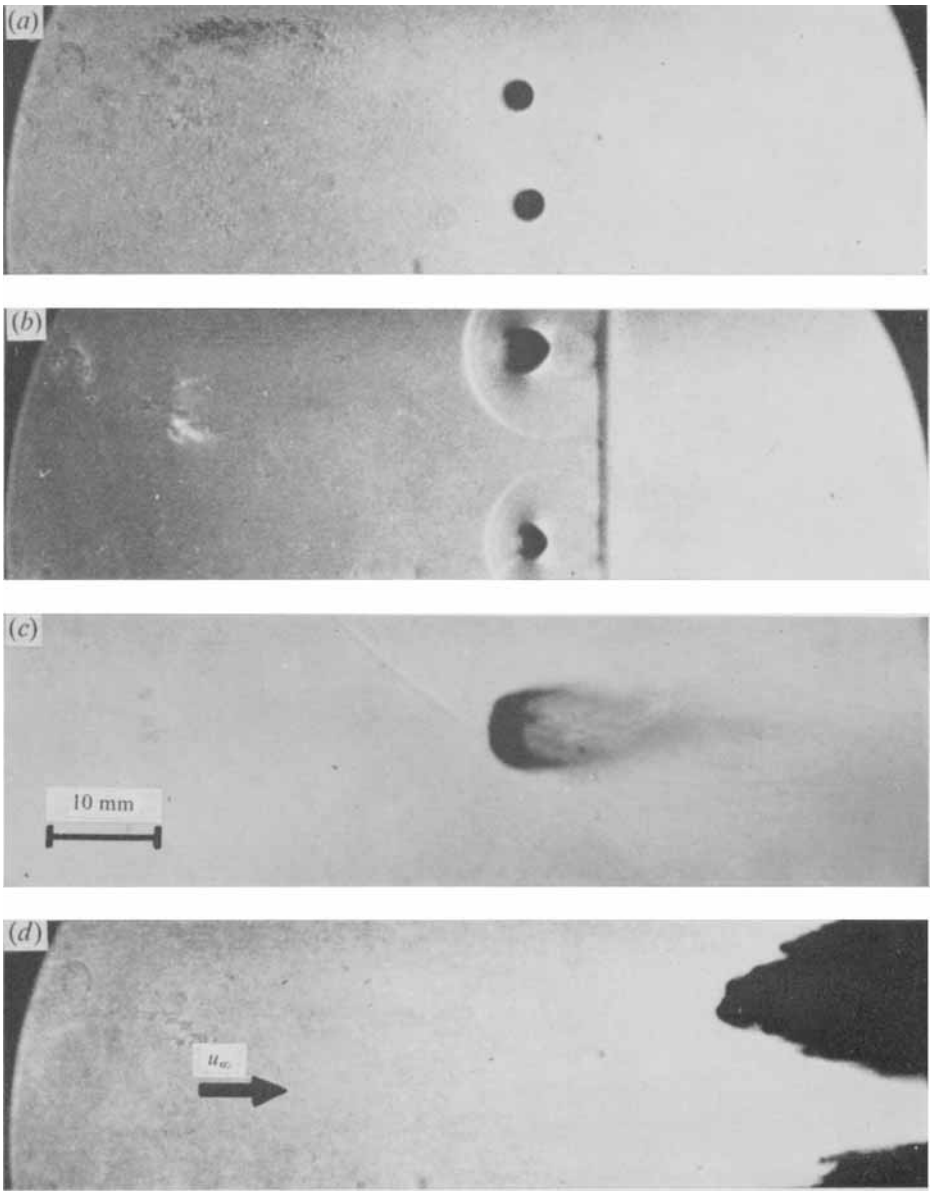

FIGURE 3. Quasi-stable response of a 2·8 mm drop in air at $Bo \simeq 1{\cdot}4 \times 10^4$. (*a*) $\bar{t} = 0$, (*b*) $\bar{t} = 11\ \mu$s, $t = \bar{t}u_2/r_0 = 3{\cdot}77$. (*c*) $\bar{t} = 70\ \mu$s, $t = 24$. (*d*) $\bar{t} = 210\ \mu$s, $t = 72$. $u_s = 0{\cdot}742$ mm/μs, $\epsilon = 3{\cdot}7 \times 10^{-3}$.

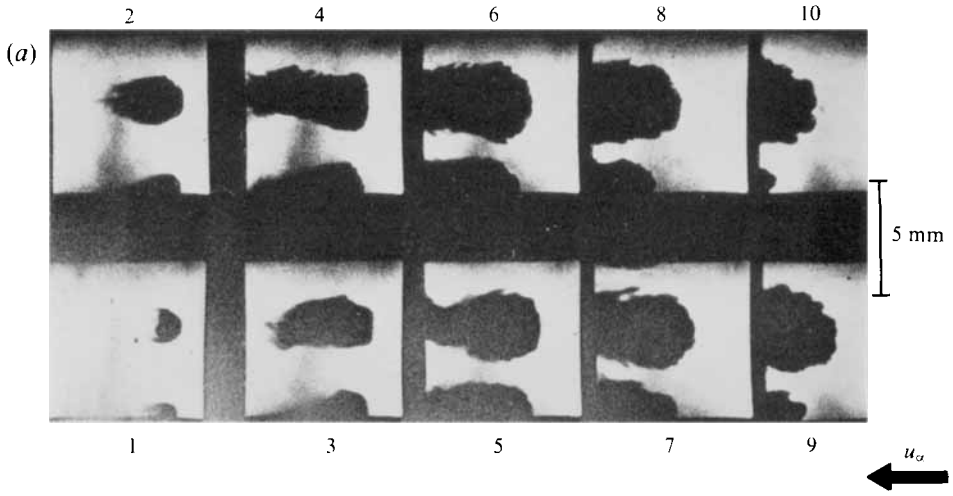

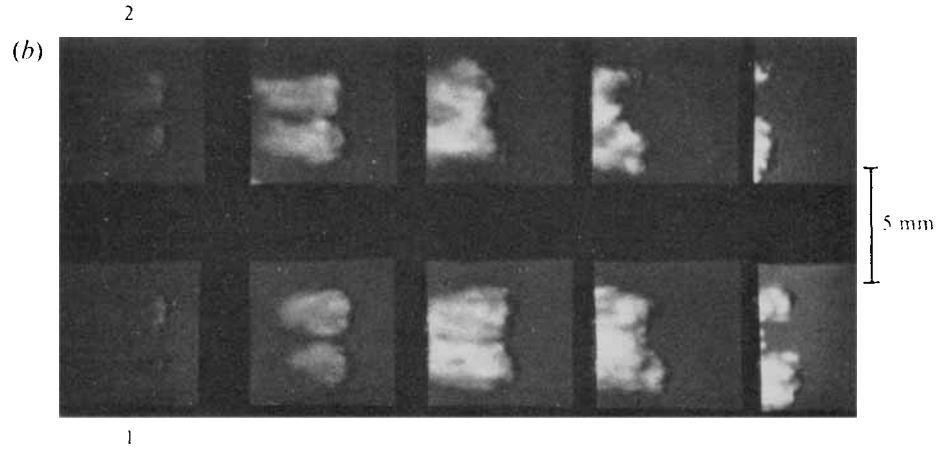

FIGURE 4. Image converter records showing the instability onset at $Bo = 5{\cdot}8 \times 10^4$, $t^* = 2{\cdot}0$ ($t \simeq 22\ \mu$s). Frame 1 taken 3 μs after impact. Framing rate $= 2 \times 10^5$/s; $M_s = 4{\cdot}80$, $u_s = 1{\cdot}58$ mm/μs, $d_0 = 1{\cdot}24$ mm. (*a*) Shadowgraph. (*b*) Front-lighted picture.